We are IntechOpen, the world's leading publisher of Open Access books Built by scientists, for scientists

6,900
Open access books available

185,000
International authors and editors

200M
Downloads

154
Countries delivered to

Our authors are among the

TOP 1%
most cited scientists

12.2%
Contributors from top 500 universities

CLARIVATE ANALYTICS
BOOK CITATION INDEX
INDEXED

WEB OF SCIENCE™

Selection of our books indexed in the Book Citation Index
in Web of Science™ Core Collection (BKCI)

Interested in publishing with us?
Contact book.department@intechopen.com

Fractal Analysis of InterMagnet Observatories Data

Sid-Ali Ouadfeul and Mohamed Hamoudi

Additional information is available at the end of the chapter

1. Introduction

The fractal analysis has been widely used in geophysics (Ouadfeul, 2006; Ouadfeul, 2007; Ouadfeul and Aliouane; 2010a; Ouadfeul and Aliouane, 2010b; Ouadfeul and Aliouane; 2011; Ouadfeul et al; 2012a, 2012b).

The purpose of this chapter is to use the fractal analysis to detect and establish a schedule of geomagnetic disturbances by analyzing data from the International Real-time Magnetic Observatory Network (INTERMAGNET) observatories. This will be achieved by the use of fractal formalism revisited by the continuous wavelet transform. Several techniques have been applied for prediction of geomagnetic disturbances. We cite, for example, the technique of neural networks for prediction of magnetic storms (Iyemori et al, 1979; Kamide et al, 1998; Gleisner et al, 1996).

In this chapter we analyze signals by the fractal formalism to predict geomagnetic storms and provide a schedule of geomagnetic disturbances. The technique of maximum of modulus of the continuous wavelet transform is used. We start the chapter by giving some definitions in geomagnetism. We then give a short description of magnetic storm and its effects. The proposed methods of analysis are then applied to data recorded by different observatories.

2. Overview of the geomagnetic field

2.1. Definitions

Earth's magnetic field or geomagnetic field is a complex electrodynamics phenomenon, variable in direction and intensity in space and time. Its characterization is useful to isolate the different geomagnetic field contributions (Merrill and Mc Elhinny, 1983). Recall that at

the Earth's surface, one can distinguish two main processes. The first one is due to the inside of the Earth (internal field) and the second one is due to the outside (external field) (Le Mouël, 1969). The internal field is presented by the main field (99%) from the measured one at the earth's surface. The geodynamo is the origin of earth magnetic field. The lithospheric anomaly filed is due to rocks magnetization located above the Curie isothermal surface. The external geomagnetic field is generated by external electric currents flowing in the ionosphere and magnetosphere.

2.2. Modelling of the geomagnetic field

Since the nineteenth and the time of Gauss, the modelling of the internal magnetic field consists to develop a synthetic mathematical expression based on the contribution of multipolar magnetic sources. This modelling is based on observations (Chapman and Bartels, 1940). The mathematical model is used either to study the core field, or to serve as reference field for exploration and navigation on the Earth's surface.

The first description of the geomagnetic field is quoted to Gauss in 1838. He used the spherical harmonic expansion to characterize the Earth's magnetic field.

In a source-free medium free of sources (e.g., between the surface of the Earth and the lowest layer of the ionosphere), one can show that the field derives from a scalar potential V following B = - grad(V). It means that this potential satisfies the Laplace equation's ΔV = 0. So the potential is harmonic and is expressed in spherical coordinates as a spherical harmonic expansion (Chapman and Bartels, 1940):

$$V(r,\theta,\varphi) = a\sum_{n=1}^{\infty}\sum_{m=0}^{n}(\frac{a}{r})^{n+1}(g_n^m(t)\cos(m\varphi) + h_n^m(t)\sin(m\varphi))P_n^m(\cos(\theta)) + a\sum_{n=1}^{\infty}\sum_{m=0}^{n}(\frac{r}{a})^{n}(q_n^m(t)\cos(m\varphi) + s_n^m(t)\sin(m\varphi))P_n^m(\cos(\theta))$$

$$\underbrace{\phantom{V(r,\theta,\varphi) = a\sum_{n=1}^{\infty}\sum_{m=0}^{n}(\frac{a}{r})^{n+1}(g_n^m(t)\cos(m\varphi) + h_n^m(t)\sin(m\varphi))P_n^m(\cos(\theta))}}_{\text{Internal Sources}}\qquad\underbrace{\phantom{a\sum_{n=1}^{\infty}\sum_{m=0}^{n}(\frac{r}{a})^{n}(q_n^m(t)\cos(m\varphi) + s_n^m(t)\sin(m\varphi))P_n^m(\cos(\theta))}}_{\text{External sources}}$$

Where:

(r,θ,φ) are the spherical coordinates, t is time and a is the mean radius of the Earth (6371.2 km). n, m, are respectively the degree and the order of development. $g_n^m(t), h_n^m(t)$ are the Gauss's internal coefficients, and $q_n^m(t), s_n^m(t)$ are the Gauss external coefficients. $P_n^m(\cos(\theta))$ are the associated Legendre polynomials semi-normalized in the sense of Schmidt.

2.3. Elements of the geomagnetic field

The geomagnetic field is a vector characterized by a direction and intensity. At any point P of the space, the geocentric components B_r, B_θ and B_φ of the geomagnetic field are connected to the geographical components X, Y and Z.

The complete determination of the field at a point P in space requires the measurement of three independent elements may be chosen from the following seven elements (Fig. 1):

1. The East component X = -B_θ.
2. The West component Y = B_φ.

3. The vertical component $Z = -B_r$.
4. Magnetic declination D may simply be defined as the azimuth of the magnetic meridian. The declination is positive when the magnetic meridian is east of geographic meridian.

The magnetic inclination I, is the angle between the direction of the field vector and its projection on the horizontal plane. It is positive when the vector field points towards the interior of the Earth (Northern Hemisphere).

5. The intensity B (or sometimes labelled T) or the module of the magnetic field is given by the following formula:

$$B = \sqrt{X^2 + Y^2 + Z^2}$$
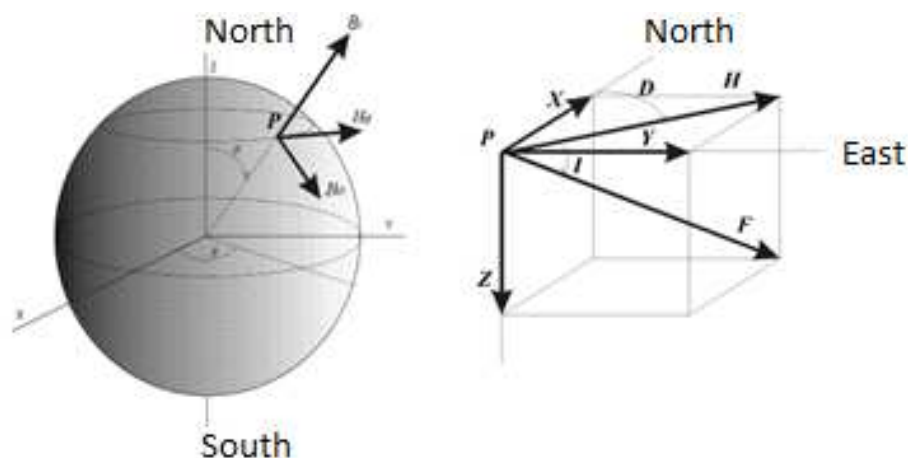
Figure 1. Elements of the geomagnetic field at a point P in the geocentric spherical coordinate system (a) and the local geographic coordinate system (b). (adapted from Blakely, 1996)

6. The horizontal component H, or any of its components horizontal, Y or X, will be particularly sensitive to external effects, such as magnetic storms.

2.4. The magnetic storms

Solar activity modulates the transient variations of the geomagnetic field. In particular, the undecennal cycle is clearly seen in the temporal distribution of sunspots as well as the magnetic activity as highlighted by the variation of the K or Dst indices. The increase in electron density due to the solar wind in different layers of the ionosphere would vary the intensity of the geomagnetic field causing many effects. The main effects (Campbell, 1997) are:

- Change the direction of the magnetic field;
- Variation of the intensity of fluctuations of the terrestrial magnetic field, mainly the horizontal component;
- Induced noise in electric cables or in the telephone;

- Disturbance of important ionospheric propagation of radio waves;
- Appearances of auroras.

There are two types of magnetic storms:

- The Storm Sudden Commencement (SSC) which is synchronous at all points of the Earth. The magnitude of the storm could reach the thousand of nT. It is more intense in the vicinity of the maxima of the solar cycles. SSCs occur few tens of hours after solar flares. It is accompanied by an intense emission of ultraviolet rays affecting the ionospheric layers D and E, in addition to showers of fast protons. The storm may last several days.
- The storm with gradual onsetwhich is characetrized by a moderate average intensity, and more localized effects. It often occurs with some regularity of the order of 27 days, corresponding to the period of intrinsic solar rotation.

Monitoring the solar activity can help to predict certain disturbances in the propagation of waves whose effects can be serious for telecommunications, as well as the impact of these storms on the distribution of electrical energy. In 1965, a massive power failure plunged the North American continent in the dark, or 30 million people out of 200 000 km2 (Campbell, 1997). In 1989, a failure of the same origin affected 6 million people in Quebec (Canada). The auroras produced by this storm were visible over Texas.
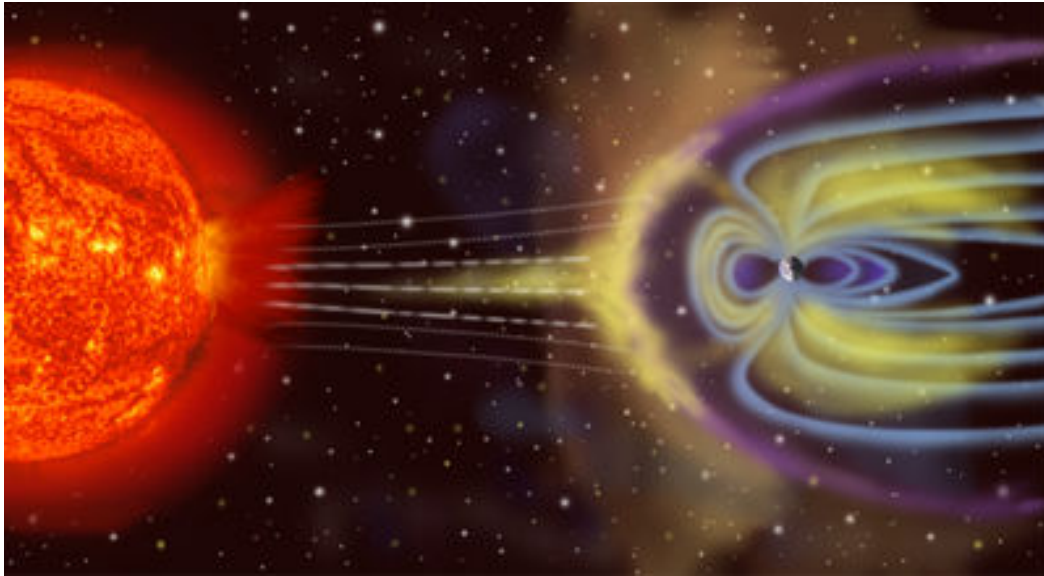

Figure 2. Interaction of the solar magnetic storm with the magnetosphere (Wékipedia).

2.5. Dst index

The geomagnetic Dst index (Menvielle, 1998) is an index that tracks the global magnetic storms. It is built by the average of the horizontal component H of the geomagnetic field measured at mid-latitude observatories. Negative values of Dst indicate a magnetic storm in progress. The minimum value of Dst indicates the maximum intensity of the magnetic storm.

3. Fractal analysis of INTERMAGNET observatories data

To analyze data from observatories, an algorithm was developed (Fig. 3). It is based on the estimation of Hölder exponents at maxima of modulus of the Continuous Wavelet Transform (CWT).
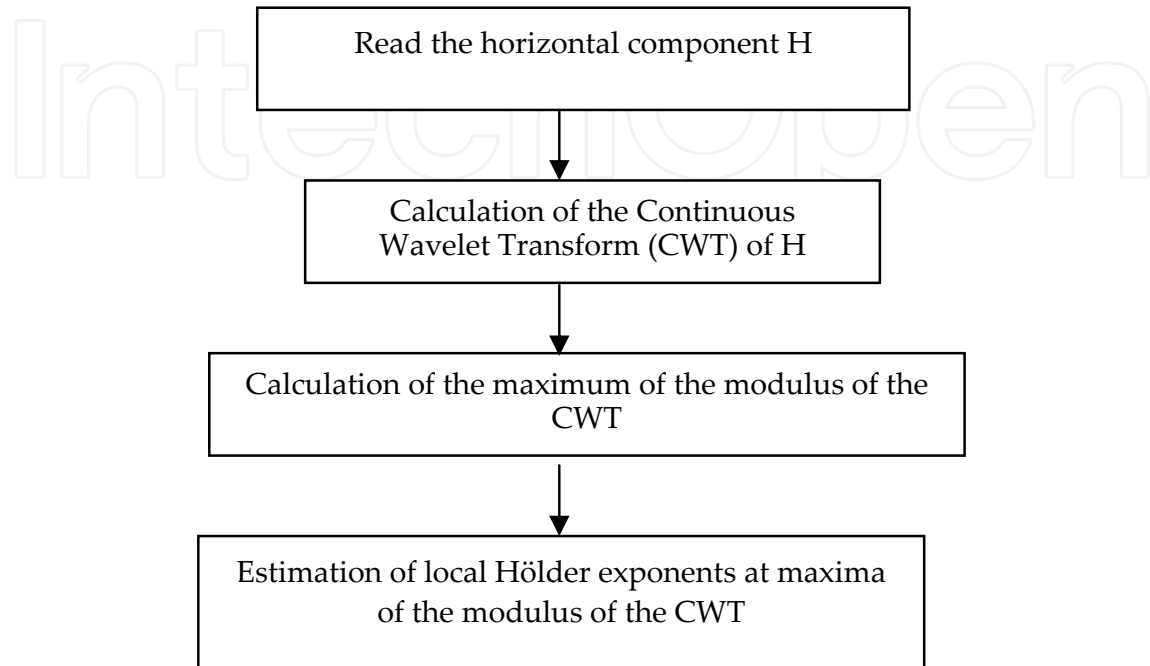
```
┌─────────────────────────────────────────┐
│     Read the horizontal component H      │
└─────────────────────────────────────────┘
                    │
                    ▼
┌─────────────────────────────────────────┐
│    Calculation of the Continuous         │
│     Wavelet Transform (CWT) of H         │
└─────────────────────────────────────────┘
                    │
                    ▼
┌─────────────────────────────────────────┐
│  Calculation of the maximum of the       │
│          modulus of the CWT              │
└─────────────────────────────────────────┘
                    │
                    ▼
┌─────────────────────────────────────────┐
│  Estimation of local Hölder exponents    │
│   at maxima of the modulus of the CWT    │
└─────────────────────────────────────────┘
```

Figure 3. Flowchart for estimating local Hölder exponents on WTMM

3.1. Wingst observatory data analysis for May 2002

We analyze the Wingst magnetic observatory (Germany) data recorded during May 2002. This period saw large geomagnetic disturbances. (See tables 1 and 2). Table 3 gives all information on the location and type of magnetometer used for Wingst observatory. We analyzed the horizontal component of the magnetic field. This last is calculated from the X and Y components. Figure 4 shows this component versus the time. The modulus of the continuous wavelet transform is shown in Figure 5.

Date	Hour	Max Hour	End Hour
11	11.21	11.32	11.41
17	15.50	16.08	16.14
20	10.14	10.29	10.34
20	10.49	10.53	10.56
20	15.21	15.27	15.31
22	17.55	23/10.55	24/14.55

a

Date	Starting Hour
11	10.13
14	xx.xx
23	1.48

b

Table 1. **a** Major solar events that could cause a perturabation; **b** Magnetic storms recorded during the month of May 2003.

Station Code	WNG
Organization	GeoForschungsZentrum, Potsdam
Co-latitude	36,257°N
Longitude	9,073 ° E
Altitude:	50 Meter
Country	Germany

Table 2. Characteristics of the Wingst observatory
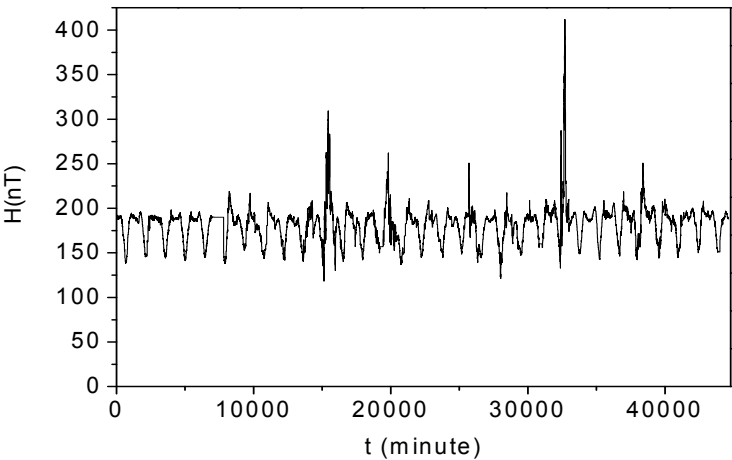
Figure 4. Horizontal component of the magnetic field recorded by the Wingst observatory during the month of May 2002.
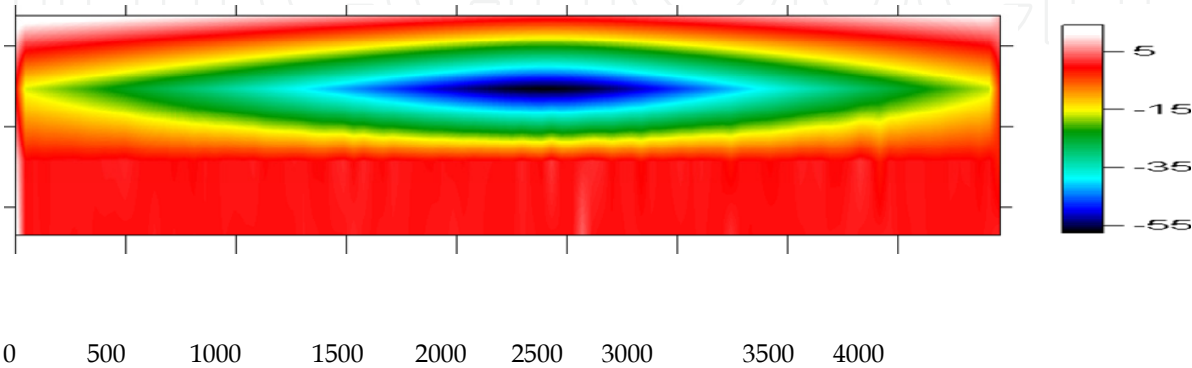
Figure 5. Wavelet Coefficients in time-log(scale) frame

The next step consists to calculate the Hölder exponents at the local maxima of the modulus of the continuous wavelet transform. Note that the calculation of Hölder exponents at maxima of the modulus of the CWT is the core of this analysis. Indeed, this is the point which can differentiate the proposed method over other methods based on the Hölder exponent estimation. This method allows us to save time by calculating the Hölder exponents only at representative times of magnetic disturbances. Figure 6 is a representation of the obtained results. To compare the obtained results with the Dst index, we calculated an average value of the Hölder exponents for each hour of the month. The obtained results are shown in Figure7.
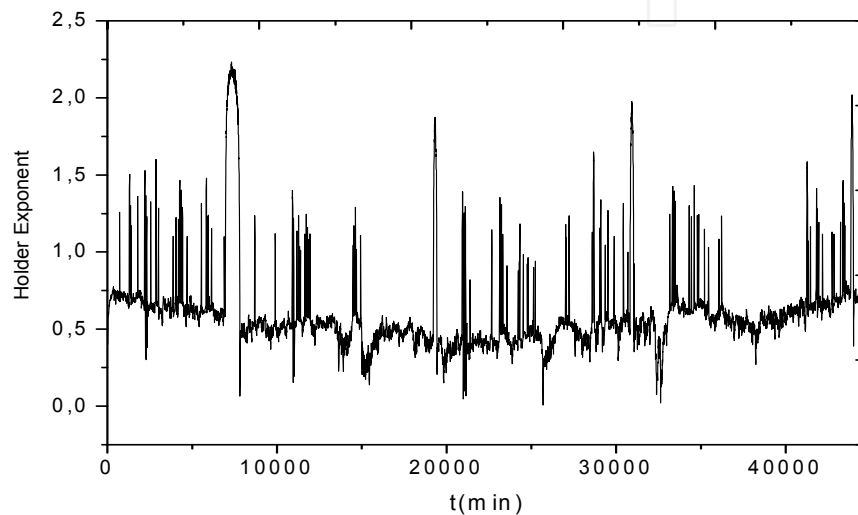
Figure 6. Estimated Hölder exponents at maxima of the modulus of the CWT.

Results and interpretation

It is clear that the horizontal component H is characterized by a Hölder exponent of very low value at the moment of the magnetic storm (Figure 7). Each event is characterized by a peak in the curve of the Dst index. Figure 8 is a detailed presentation between days 8 to 13, showing the behaviour of the Hölder exponent before, during and after the magnetic storm. We observe that hours before the storm are characterized by progressive decrease of the Hölder exponent to reach the minimum value h = 0.07 at t = 11.55day (11th day and 13.20 hours). After the storm, we observe a gradual increase of the Hölder exponent.

3.2. Baker Lake observatory data analysis

We analyzed the horizontal component recorded by the Baker Lake Observatory for May 2002. The observatory's informations are given in table 4.

Figure 9 presents the horizontal component of the magnetic field and figure 10 presents the average local Hölder exponents for each hour of the month compared with the Dst index. We note that the major magnetic storms are characterized by negative values of the Dst index and by very low values of the Hölder exponents.
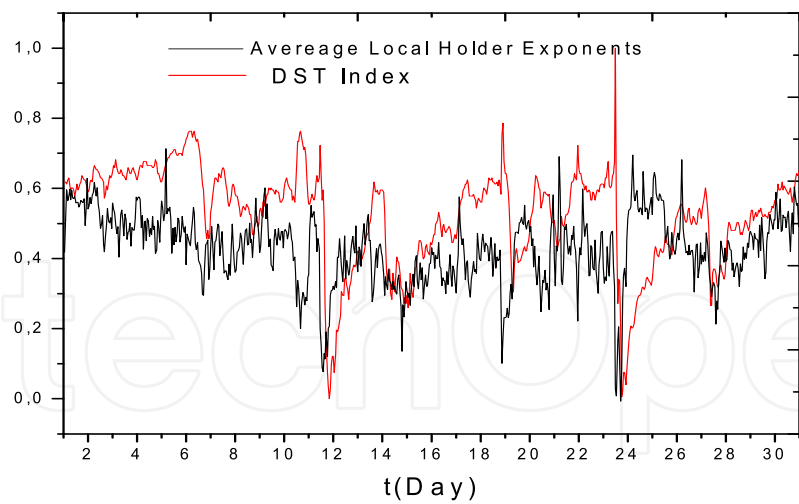
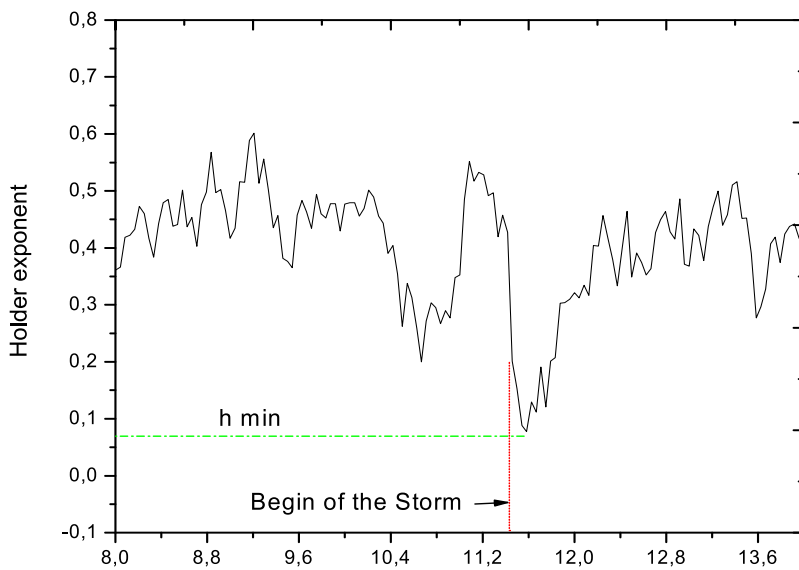**Figure 7.** Average Hölder exponents compared with the Dst index .

Figure 8. Variation of the Hölder exponent between days 8 and 13
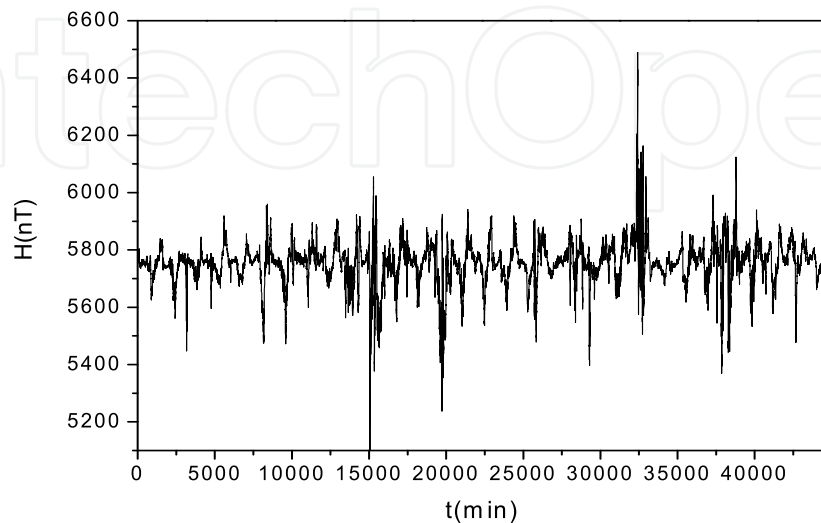

Figure 9. Horizontal component recorded by the Baker Lake Observatory during May 2002.
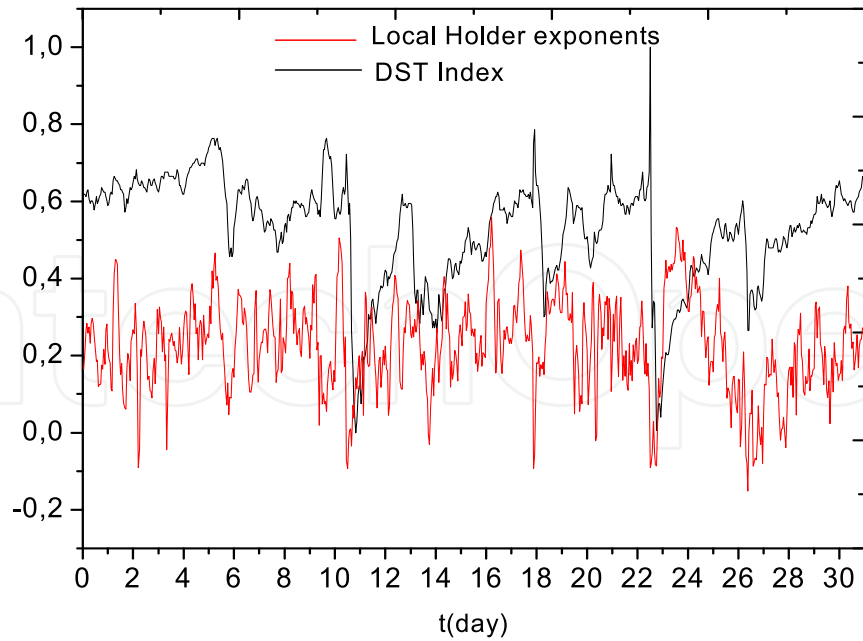
Figure 10. Local Hölder exponents mean calculated every hour and compared to the Dst index.

4. Demonstration of the multifractal character of the signal of the external geomagnetic field

The WTMM can distinguish between monofractal and multifractal (Arnéodo et al., 1988; Arnéodo and Bacry, 1995). We will use this feature to demonstrate the multifractal character of the external geomagnetic field. Data analysis of the total field recorded by the Wingst observatory during the month of May 2002 by the WTMM technique gives a spectrum of exponents and a spectrum of singularities that demonstrate the multifractal character of the external geomagnetic field signals. (See figure11). Indeed, the spectrum of exponents is not linear and the spectrum of singularities is not concentrated at one point.
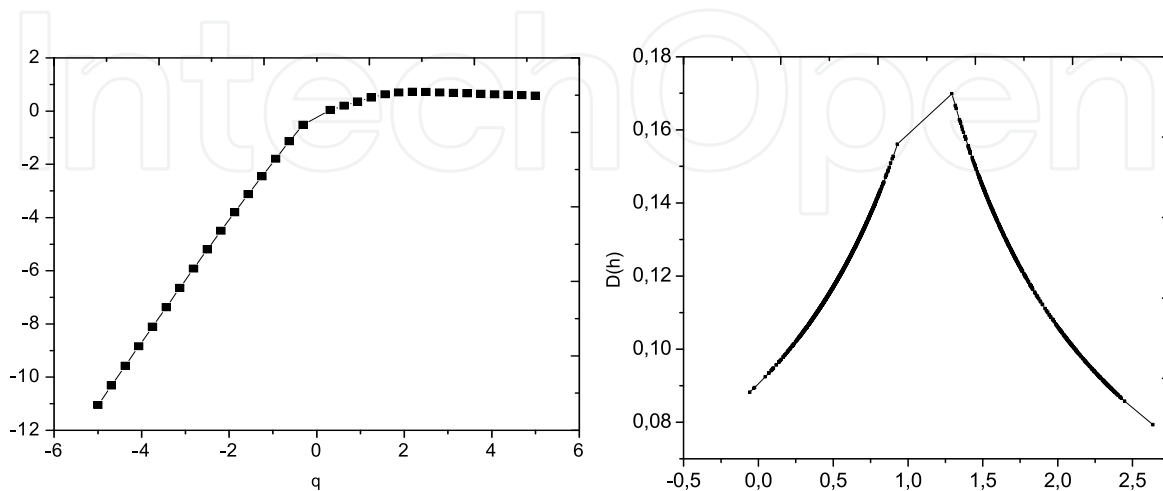
Figure 11. Multifractal analysis of the external geomagnetic field for the period of May 2002.
(a) Spectrum of exponents. (b) Spectrum of singularities.

5. The generalized fractal dimensions as an index of magnetic disturbances

In this section we will demonstrate the usefulness of generalized fractal dimension D(q) to establish a calendar of magnetic disturbances. We will apply this technique at the data of many InterMagnet observatories data. Two important periods are analyzed. One is the month of May 2002 and the second is the period of October and November 2003.5.1 Data Analysis of the period of May 2002

5.1.1. Analysis of data of Hermanus observatory

The first record to be processed is the total field recorded by the Hermanus observatory during the period of May 2002. The total field variations are shown in Figure 12.

Station Code	HER
Localisation	Hermanus
Organisation	National Research Foundation
Co-latitude	124,425°
Longitude	019,225°E
Altitude	26 m
Country	South Africa

Table 3. Characteristics of Hermanus observatory.

$$D(q) = \frac{\tau(q)}{(q-1)}$$
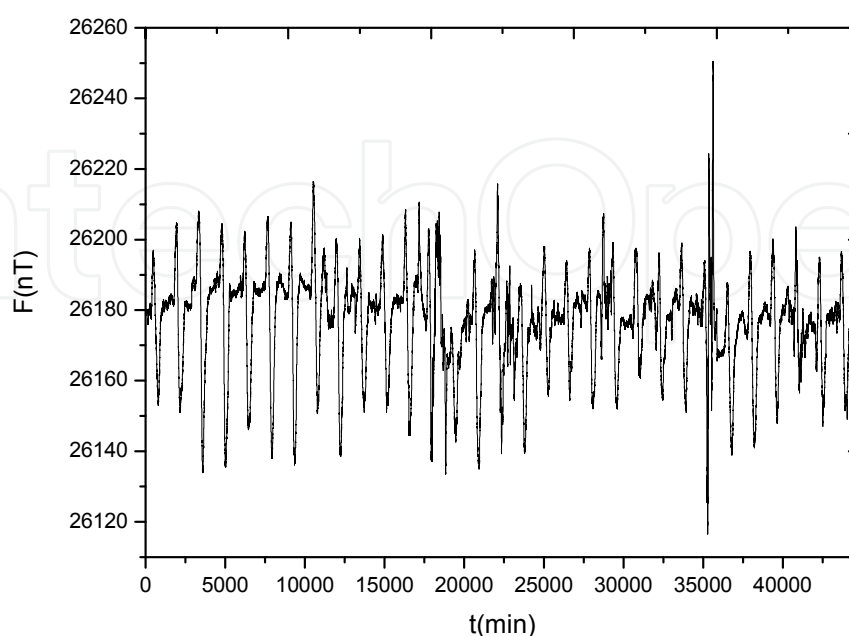
Figure 12. Total magnetic field recorded during May 2002 by the Hermanus observatory.

The first step is to apply the WTMM technique on data of each hour of the month, that is to say, every 60 samples. The objective is to estimate the spectrum of exponents τ (q). Then we compute the generalized fractal dimensions for the following values of q: 0, and 2. The following formula is used (Ouadfeul et al, 2012):

$$D(q) = \frac{\tau(q)}{(q-1)}$$

Note that for D (1) we use the limit of D (q) when q tends towards 1.
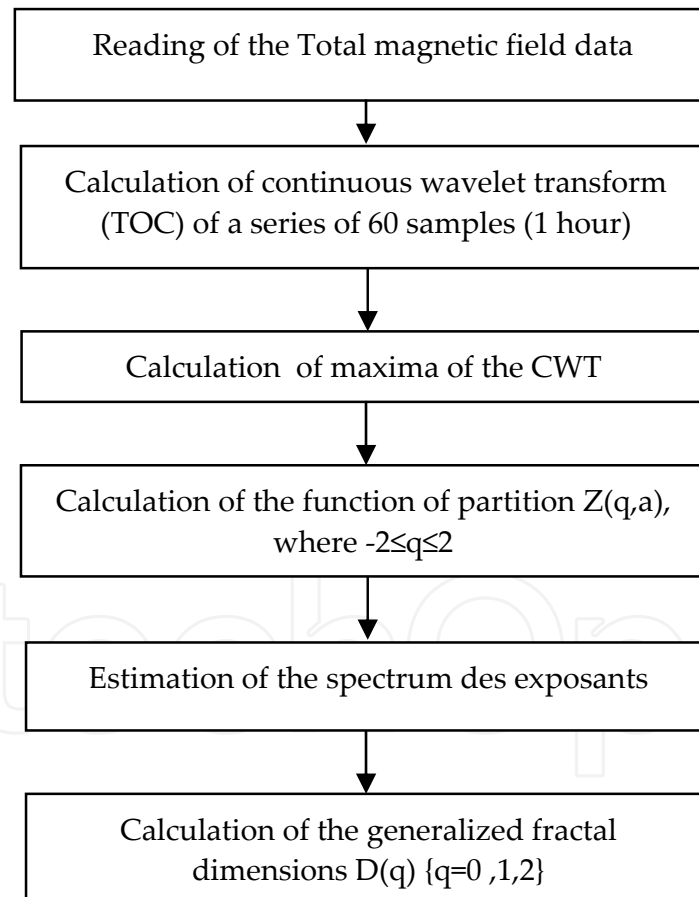
Figure 13 presents of the flow chart of the proposed technique.

Figure 13. Flowchart of the total magnetic field analysis using the generalized fractal dimensions.

Application of the WTMM method at the first 60 samples of the total field is shown in figure 14.
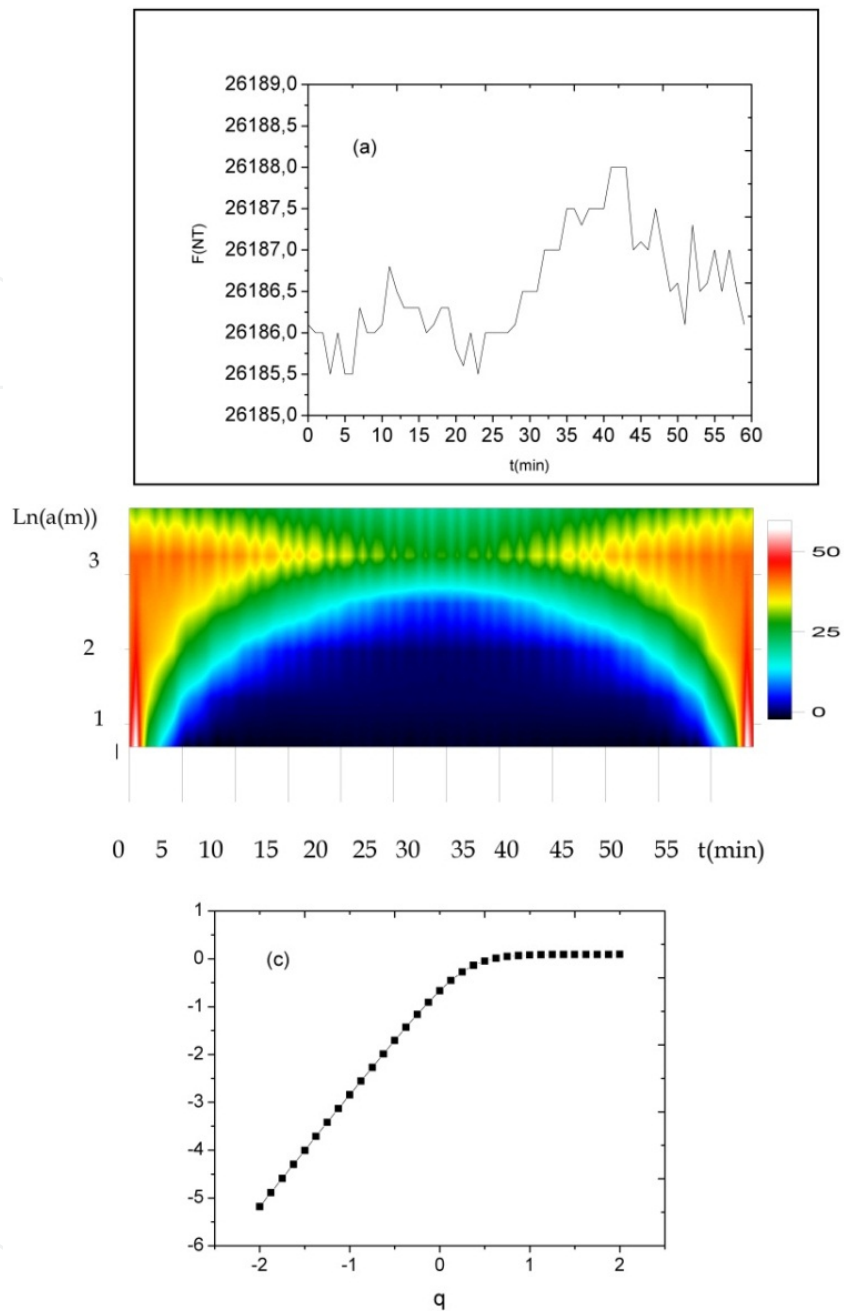
Figure 14. WTMM analysis of 60 samples of total magnetic field intensity recorded during May 2002 at Hermanus observatory.
(a) Recorded signal. (b) Wavelet coefficients.(c) Spectrum of exponents.

The same operations are applied to each hour of May 2002. Fractal dimensions are then calculated. The obtained results are shown in figure 15

Results and interpretation

Obtained results show the non sensitivity of the fractal dimension D_0 to the magnetic disturbances. However, for the generalized fractal dimensions D_1 and D_2, the main magnetic disturbances are characterized by peaks (see Tables 1a and 1b and figure 14).
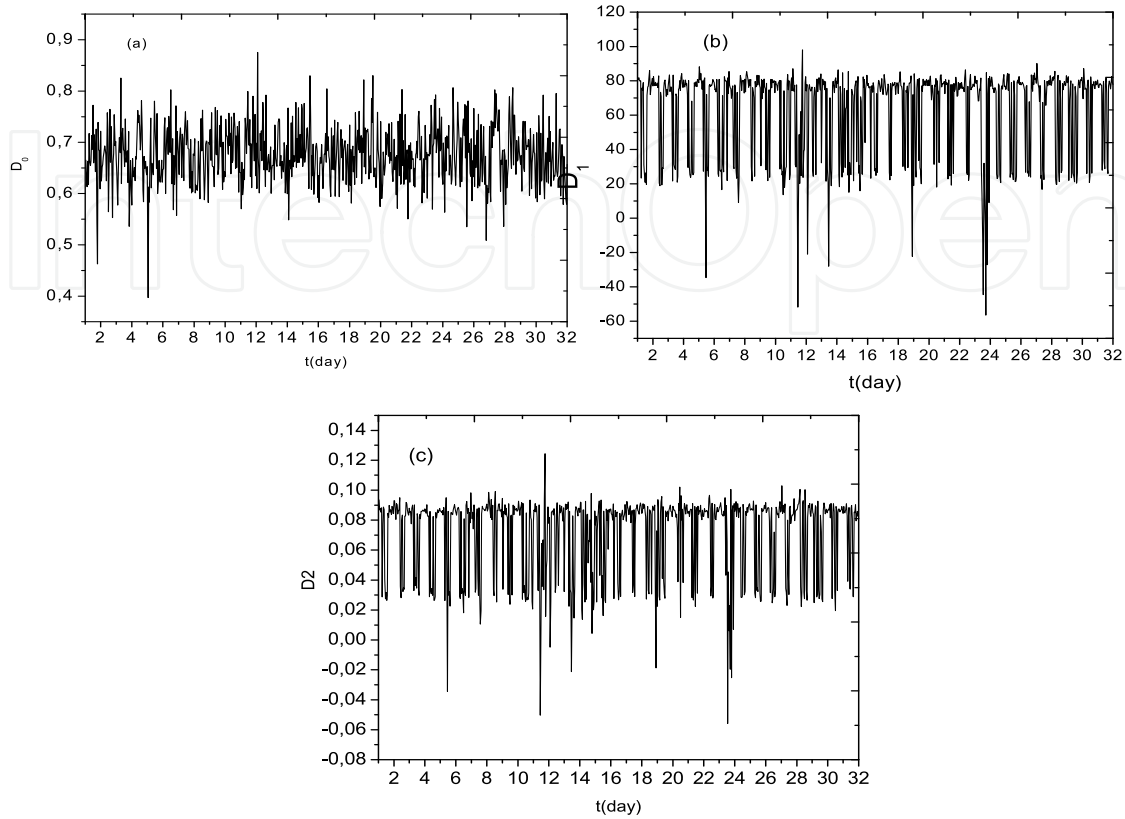
Figure 15. Fractals dimensions estimated at every hour of May 2002 (Hermanus Observatory)
(a) D_0, (b) D_1, (c) D_2

The obtained results show that peaks are observed in the generalized fractal dimensions D_1 and D_2 at the times of occurrences of magnetic storms. These dates correspond to 11, 14 and 23 of May 2002. One can notice that the dimension D_0 is not clearly sensitive to the magnetic storm.

5.1.2. Baker Lake observatory data analysis

We analyzed by the same way the signal of magnetic field intensity recorded by the Baker Lake Observatory during May 2002. Figure 16 shows the fluctuations of this field with time.

The generalized fractal dimensions are calculated at each hour of the month. The obtained results are shown in Figure 17. We note that peaks are observed in the plot of D_1 and D_2 at the time of the magnetic storms (Tables 1a and 1b).
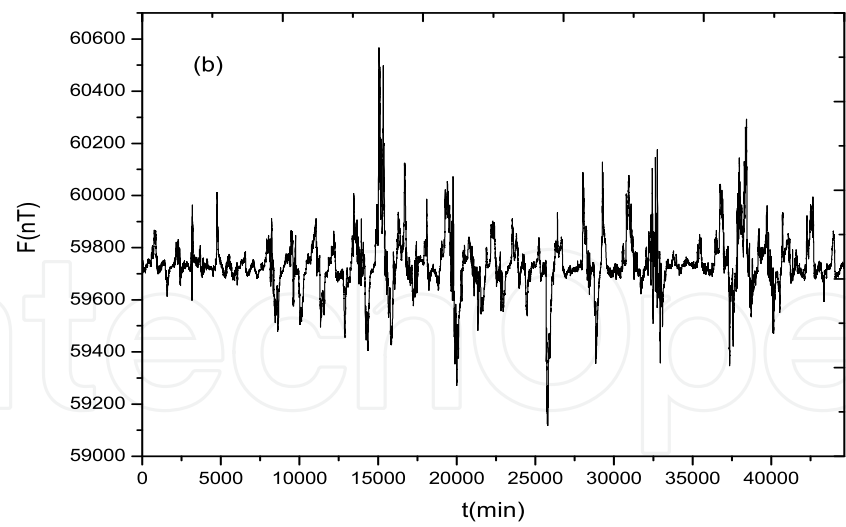
Figure 16. Total field recorded during May 2002 by the Baker Lake observatory

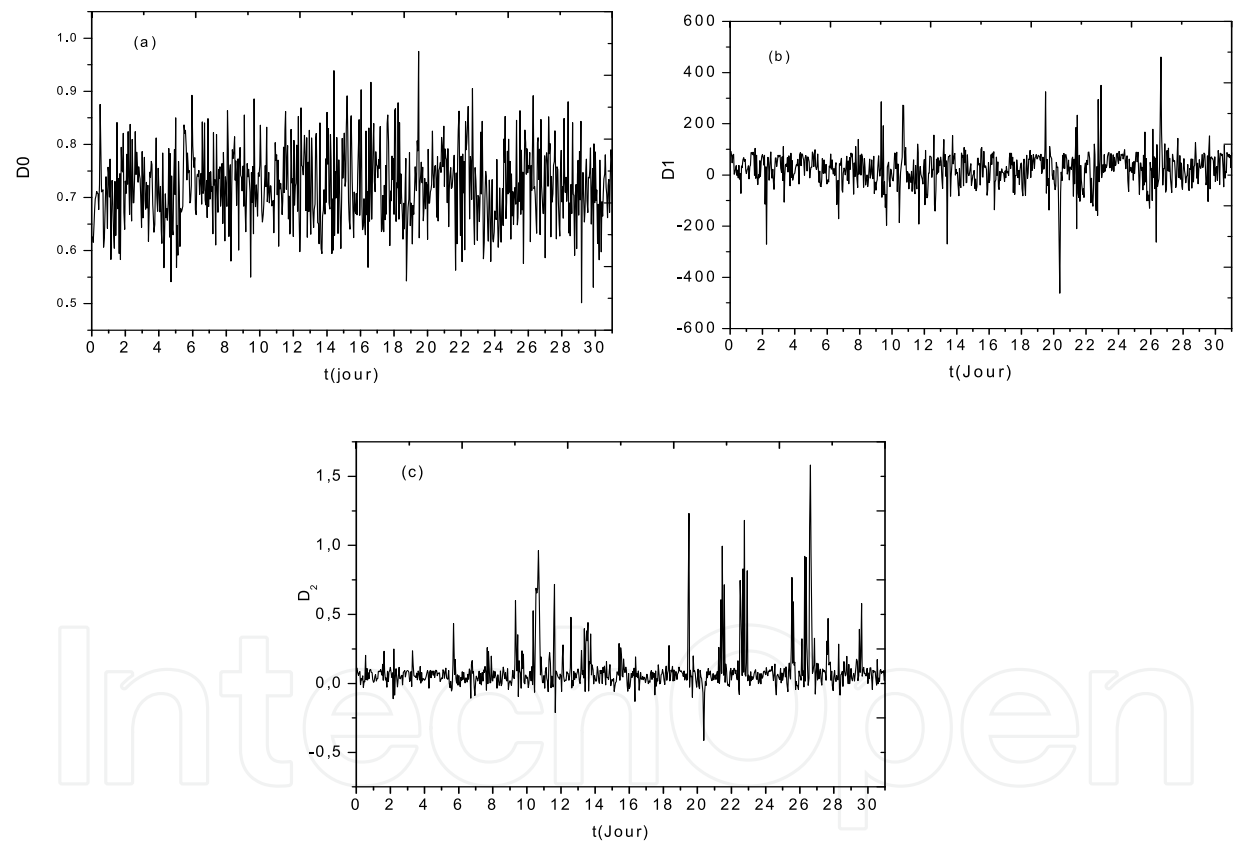**Figure 17.** Generalized fractal dimensions calculated for each hour of the month of May 2002, of the Baker Lake observatory (a) D_0 (b) D_1 (c) D_2

5.2. Analysis of geomagnetic data for months of October and November 2003

5.2.1. Data analysis from the Kakioka observatory

We analyzed the total field recorded by the Japanese Kakioka observatory, the details of this observatory are summarized in table5. Figure 18 shows the total magnetic field fluctuations

during the months of October and November 2003. The generalized fractal dimensions are shown in figure 19.

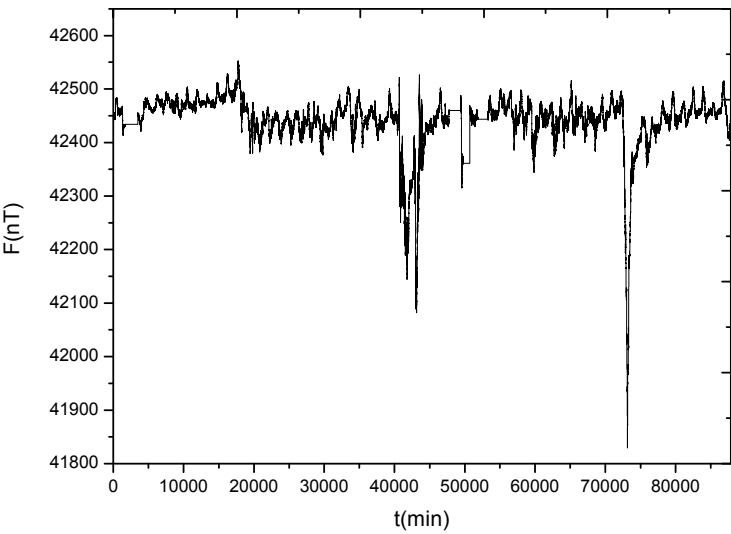| Station Indicative	KAK
Localisation	Kakioka, Japan
Organisation:	Japan Meteorological Agency
Co-latitude:	53,768°
Longitude:	140,186°E

Table 4. Characteristics of the Kakioka observatory

Figure 18. Total field recorded by the Kakioka observatory during October and November 2003
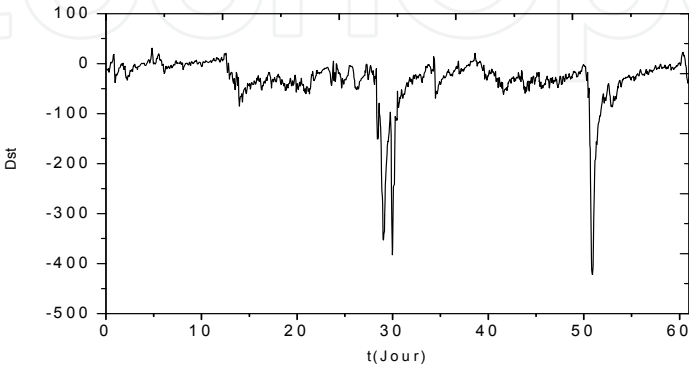

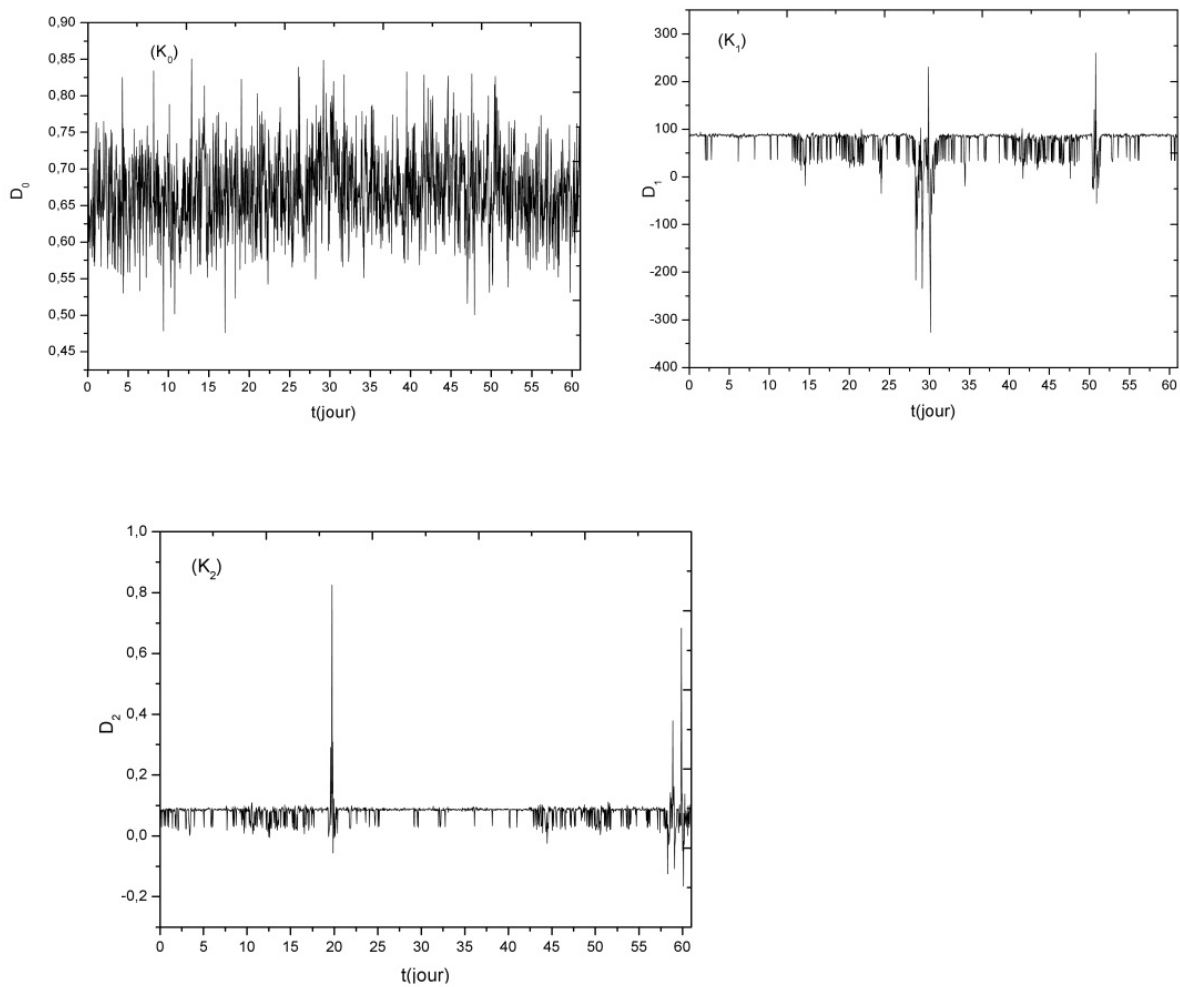**Figure 19.** Dst Index calculated during the period of October and November 2003

Figure 20. Generalized fractal dimensions calculated during October and November 2003. $K_1 : D_0$; $K_1 :$ D_1 ; $K_2 : D_2$

Results analysis shows that in moments of the magnetic storm we observe significant spikes in the graphs of generalized fractal dimensions D_1 and D_2 (see figure 19 and tables 5 and 6) . The generalized fractal dimension D_0 is not sensitive to geomagnetic disturbances.

Date	Begin Hour
14	18.23
19	xx.xx
21	16.53
24	xx.xx
29	06.09
30	21.16

Table 5. Magnetic storms recorded during October 2003

Date	Begin Hour
04	06.24
06	19.33
09-18	xx.xx
20	08.02
23	16.34

Table 6. Magnetic storms recorded during November 2003

5.2.2. Data analysis of the Hermanus observatory

We analyzed by the same way, data of Hermanus observatory. Figure 21 shows the total field recorded during the months of October and November 2003. The generalized fractal dimensions are calculated using the WTMM method. Figure 22 shows the fluctuations of fractal dimensions estimated by multifractal analysis method. The same phenomena are observed in the plots of generalized fractal dimensions.
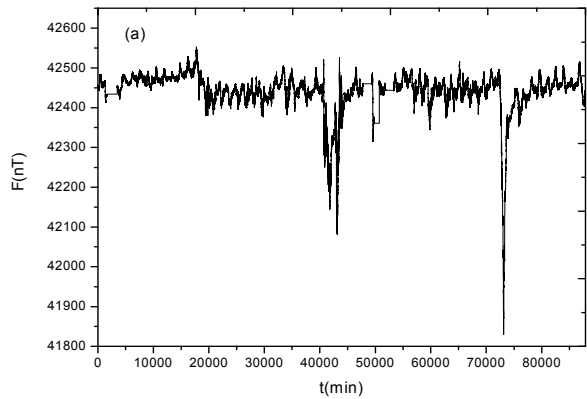

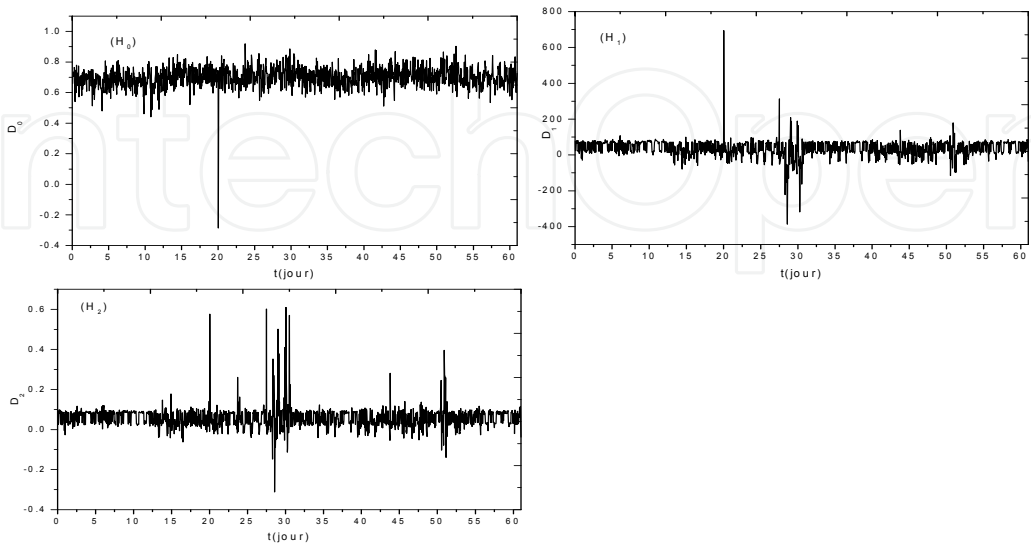**Figure 21.** Total field recorded by Hermanus observatory during October and November 2003

Figure 22. Generalized fractal dimensions calculated using data of October and November 2003 (Hermanus Observatory).

5.2.3. Analysis of data from the Alibag observatory

We also analyzed data recorded during the months of October and November 2003 by the Indian observatory Alibag,. Table 7 presents informations about this INTERMAGNET observatory. The recorded total field is shown in figure 23. The fractal dimensions are shown in figure 24.

Station (ID)	ABG
Localisation	Alibag
Organisation	Indian Institute of Geomagnetism (India)
Co-latitude	71.380°
Longitude	72.870°E
Country	India

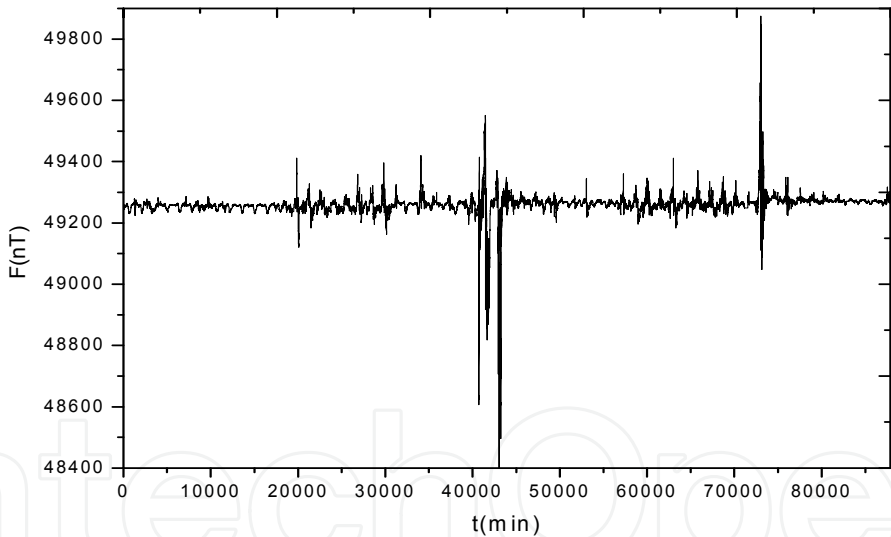**Table 7.** Characteristics of the Alibag Observatory

Figure 23. Total field recorded at Alibag observatory during October and November 2003

5.2.4. Analysis of data from the Wingst observatory

We analyzed the total field recorded by the Wingst observatory during October and November 2003. Figure 25 is presents the fluctuations of this field. The generalized fractal dimensions are shown in Figure 26. One can easily observe spikes in the generalized fractal dimensions at the times of magnetic storms. The analysis shows that the fractal dimensions D_1 and D_2 are very sensitive to geomagnetic disturbances. However the capacity dimension D_0 is not sensitive to magnetic disturbances. (See figure.26 and tables 5 and 6).
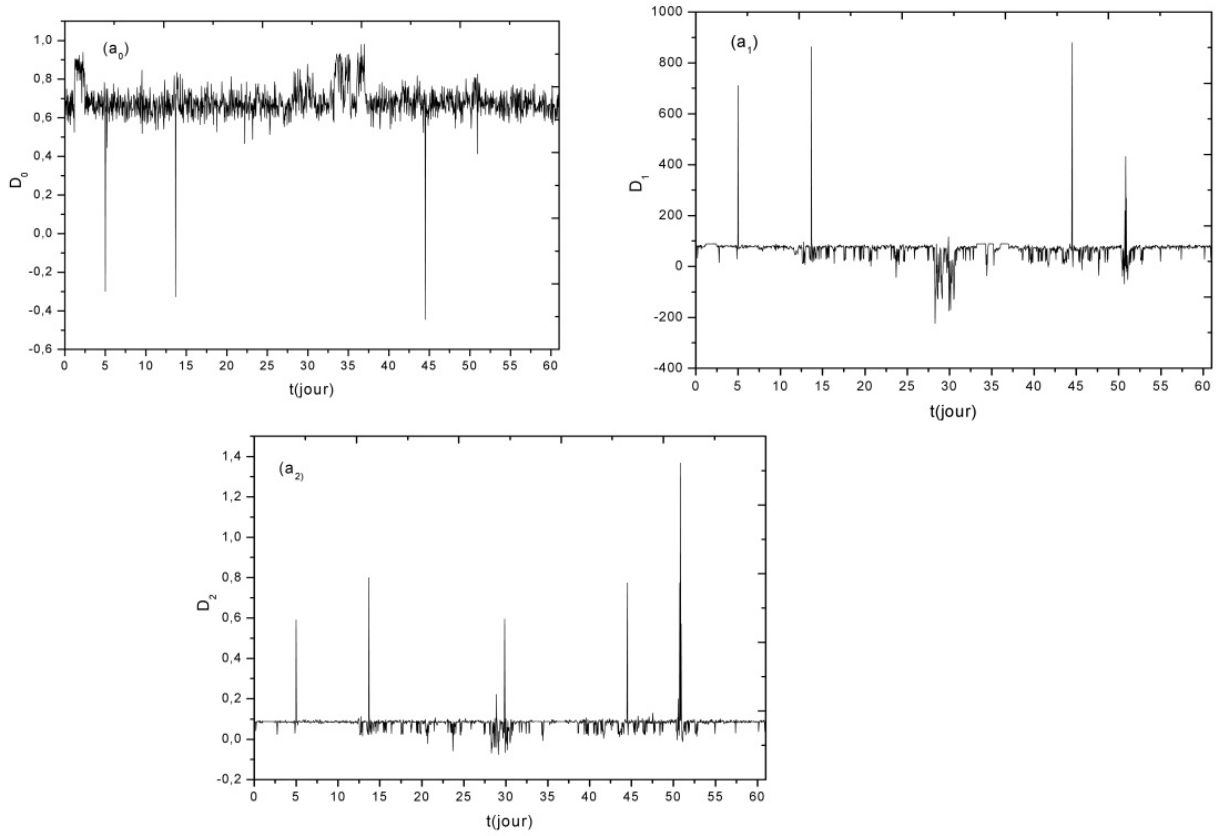
Figure 24. Generalized fractal dimensions calculated during October and November 2003 (Alibag Observatory).
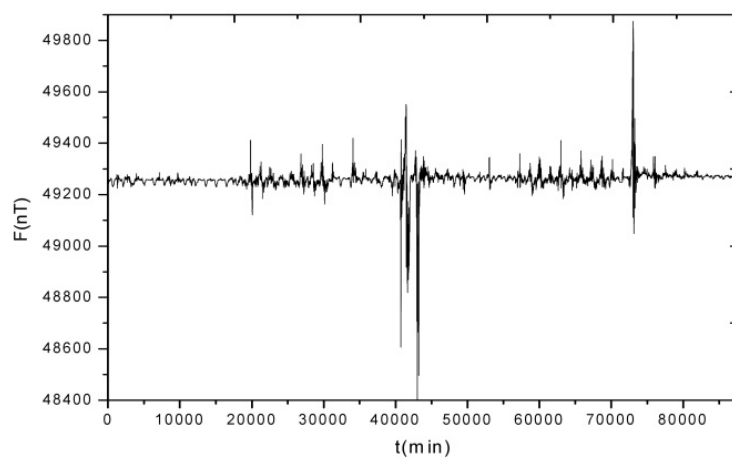

Figure 25. Total Magnetic field recorded by Wingst Observatory during October and November 2003.
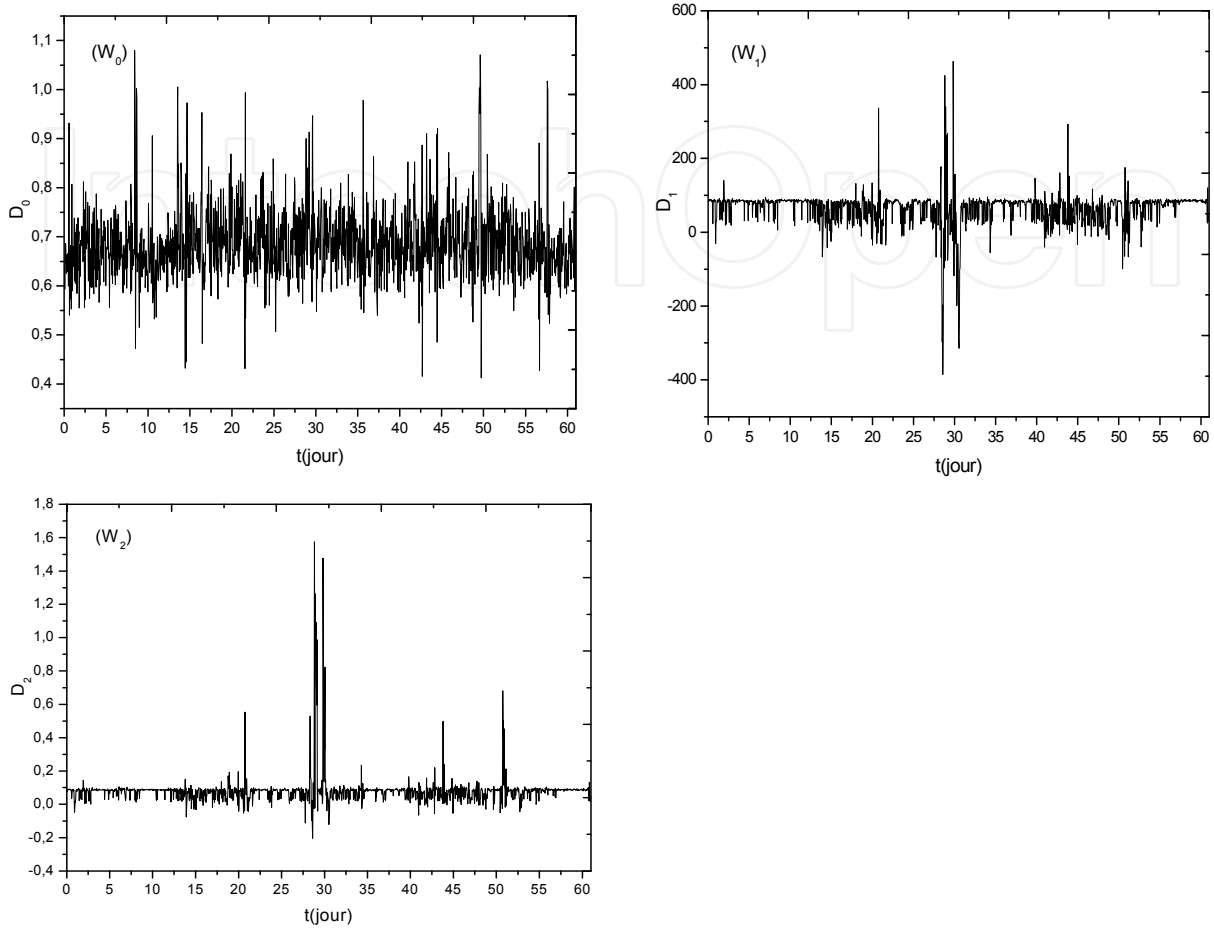
Figure 26. Generalized fractal dimensions derived from data recorded during the months of October and November 2003 (Wingst Observatory). $W_1 : D_0$; $W_1 : D_1$; $W_2 : D_2$

6. Results, discussion and conclusion

During a magnetic storm, the Hölder exponent of the horizontal component H has a very low value. Before the storm we observe gradual drop of the Hölder exponent. Several numerical experiments realized using vertical component Z recorded by magnetic observatories show that, as expected, this component is not sensitive to the magnetic disturbances. We show however that the generalized fractal dimensions D_1 and D_2 of the total magnetic field B can be confidently used as an index to describe the external magnetic activities. WTMM analysis of the horizontal component recorded during May 2002 show that this last exhibits a multifractal behaviour. This is in accordance with the analysis shown in (Ahn et al, 2007; Bolzan et al., 2009; Bolzan and Rosa, 2012). We note that these fractal dimensions show more details of solar activity compared to the Dst index. The WTMM method shows clearly the multifractal character of the signal of the geomagnetic field.

Author details

Sid-Ali Ouadfeul
Geosciences and Mines, Algerian Petroleum Institute, IAP, Algeria
Geophysics Department, FSTGAT, USTHB, Algeria

Mohamed Hamoudi
Geophysics Department, FSTGAT, USTHB, Algeria

7. References

[1] Blakely, R. J., Potential Theory in Gravity & Magnetic Applications, Cambridge University Press, 1996.

[2] Iyemori. T., Maeda. H. and Kamei. T. (1979). Impulse response of geomagnetic indices to interplanetary magnetic fields, J. Geomag. Geoelectr., 31, 1-9.

[3] Kamide. Y, Yokoyama. N, Gonzalez. W, Tsurutani. B. T, Daglis. I. A, Brekke. A., and Masuda. S.(1998)., Two step development of geomagnetic storms, J. Geophys. Res., 103, 6917– 6921.

[4] Gleisner. H and Lundstedt. H, (1997). Response of the auroral electrojets to the solar wind modeled with neural networks, J. Geophys. Res.,102, 14269–14278.

[5] Merrill, R.T., and Mc Elhinny, M.W., The Erath's Magnetic Field, Its History, Origin and Planetary Perspective, Academic Press, London (1983).

[6] Menvielle. M, (1998). Derivation and dissemination of geomagnetic indices, Revista Geofisica, 48, 51-66, 1998.

[7] Campbell, K. W. (1997), Empirical near-source attenuation relationships for horizontal and vertical components of peak ground acceleration, peak ground velocity, and pseudo-absolute acceleration response spectra, Seismological Research Letters, 68(1), 154 -179.

[8] Ouadfeul, S., (2006). Automatic lithofacies segmentation using the wavelet transform modulus maxima lines (WTMM) combined with the detrended fluctuation analysis (DFA), DFA, 17 the International geophysical congress and exhibition of turkey , Expanded abstract .

[9] Ouadfeul, S., (2007). Very fines layers delimitation using the wavelet transform modulus maxima lines WTMM combined with the DWT, SEG SRW.

[10] Ouadfeul, S., Aliouane, L, (2010a). 3D Seismic AVO Data Established by the Wavelet Transform Modulus Maxima Lines to Characterize Reservoirs Heterogeneities, 72nd EAGE Conference & Exhibition.

[11] Ouadfeul, S., Aliouane, L., (2010b). Wavelet Transform Modulus Maxima Lines Analysis of Seismic Data for Delineating Reservoir Fluids, Geo2010, Expanded Abstract.

[12] Ouadfeul, S., Aliouane, L., (2011). Multifractal Analysis Revisited by the Continuous Wavelet Transform Applied in Lithofacies Segmentation from Well-Logs Data, International Journal of Applied Physics and Mathematics vol. 1, no. 1, pp. 10-18.

[13] Ouadfeul, S., Hamoudi, M., Aliouane, L., (2012a). A wavelet-based multifractal analysis of seismic data for facies identification. Application on the pilot KTB borehole, Arabian Journal for Geosciences.

[14] Ouadfeul, S., Aliouane, L., Hamoudi, M., Boudella, A., and Eladj, S., (2012b). 1D Wavelet Transform and Geosciences, Wavelet Transforms and Their Recent Applications in Biology and Geoscience, Dumitru Baleanu (Ed.), ISBN: 978-953-51-0212-0, InTech.

[15] Blakely, R. J., (1996) Potential Theory in Gravity & Magnetic Applications, Cambridge University Press.

[16] Le Mouël. J.-L, 1969, Sur la distribution des éléments magnétiques en France. Thèse de la Faculté des Sciences de l'Univ. de Paris.

[17] Anh, V., Yu, Z.-G., and Wanliss, J. A., (2007), Analysis of global geomagnetic variability, Nonlin. Processes Geophys., 14, 701-708, doi:10.5194/npg-14-701-2007.

[18] Bolzan, M. J. A., Rosa, R. R., and Sahai, Y., 2009, Multifractal analysis of low-latitude geomagnetic fluctuations, Ann. Geophys., 27, 569-576, doi:10.5194/angeo-27-569.

[19] Bolzan, M. J. A. and Rosa, R. R., (2012), Multifractal analysis of interplanetary magnetic field obtained during CME events, Ann. Geophys., 30, 1107-1112, doi:10.5194/angeo-30-1107-2012.